Preprints of the 21st IFAC World Congress (Virtual)
Berlin, Germany, July 12-17, 2020

Robust Interval Observer Design for Fractional-Order Models with Applications to State Estimation of Batteries

Erik Hildebrandt * **Julia Kersten** ** **Andreas Rauh** **
Harald Aschemann **

* *University of Rostock, Chair of Technical Dynamics, Justus-von-Liebig-Weg 6, D-18059 Rostock, Germany (e-mail: Erik.Hildebrandt@uni-rostock.de)*
** *University of Rostock, Chair of Mechatronics, Justus-von-Liebig-Weg 6, D-18059 Rostock, Germany (e-mail: {Julia.Kersten, Andreas.Rauh, Harald.Aschemann}@uni-rostock.de)*

Abstract: Interval observers have been investigated by many researchers during the last decade, especially for those classes of systems that can be described by finite-dimensional continuous-time ordinary differential equations, discrete-time difference equations, and sets of partial differential equations in which both, system parameters and external disturbances, may be subject to bounded uncertainty. In contrast to this, only preliminary investigations were performed for fractional-order models. Due to the fact that many electro-chemical processes such as the charging and discharging dynamics of batteries can be described in good accuracy by using fractional-order models, this paper focuses on the design and numerical validation of interval observers for such systems. Here, we present a cooperativity-enforcing observer structure leading directly to decoupled lower and upper bounding systems for the sets of reachable states. This is visualized by a battery model with interval uncertainty in the output equation.

Keywords: Uncertain dynamic systems, Fractional-order dynamics, Robust state estimation, Observers, Energy storage, Convex optimization.

1. INTRODUCTION

Interval observers are powerful tools for enclosing those sets of reachable states that can be reached by a dynamic system with bounded uncertainty in the state equations as well as bounded measurement noise (Raïssi and Aoun, 2017). Despite the fact that interval observers are well explored for classical ordinary as well as partial differential equations, their application to fractional-order system models is yet a topic for which further developments are necessary to bridge the gap between existing theoretical results and real-life industrial applications. Suitable applications can be found for electro-chemical systems, where, for example, the estimation of the state of charge (SOC) of batteries as an energy storage is crucial for the implementation of reliable monitoring systems, model-based aging detection, and the implementation of robust and highly efficient power management concepts. As described in Erdinc et al. (2009) and Wang et al. (2017), batteries can be modeled either by using electric equivalent circuits with a finite number of SOC-dependent RC-subcircuits or alternatively by state-space representations which contain a finite number of fractional-order constant phase elements. Here, especially the latter approach allows for tightly fitting frequency responses that are obtained experimentally by impedance spectroscopy methods. From a system theoretic point of view, the first option mentioned before can be interpreted as a finite-dimensional truncation of the infinite horizon memory property associated with the latter fractional-order models (Podlubny, 1999; Oustaloup, 1995). In addition to these low-order, usually real-time capable models, also electro-chemical representations focusing on dynamic effects on a microscopic scale exist. However, the required computational complexity of such battery models typically prevents their usage in the frame of the application scenarios mentioned above.

To make interval observers applicable to the task of SOC estimation for batteries by using readily available data such as terminal currents (as the system input) and measured terminal voltages, interval observers are designed firstly for point-valued system models and secondly for fractional-order state-space representations with bounded (i.e., interval) uncertainty in the state equations and the disturbance model for the measured system output. For that, we employ design conditions stated in terms of linear matrix inequalities (LMIs) which directly enforce cooperative, positive error dynamics of the observer, cf. Raïssi and Efimov (2018). In such a way, it becomes possible to evaluate lower and upper bounding trajectories for each component of the state vector in a decoupled form. The prerequisite for this is the Metzler structure of the dynamic matrices of the designed state observers. Although such kind of structure may exist in the frame of battery models, the associated structural restrictions go along with a reduction of the available degrees of freedom that can be used for enhancing the tracking behavior of the observer (in terms of short transient operating phases) and for achieving insensitivity of the computed estimates with respect to noise. The latter aspect was addressed, e.g. by Ichalal et al. (2018), where despite bounded noise, the observer gain was optimized by an H_∞ methodology dealing with random disturbances within the prespecified error bounds.

In Sec. 2, preliminaries with respect to the system description, controllability, observability, and stability analysis of fractional-order linear time-invariant models (FLTI) are given. Sec. 3 summarizes the aforementioned procedures for the interval observer design of FLTI models, before numerical simulations are presented in Sec. 4 to highlight the practical applicability in the frame of SOC estimation for Lithium-Ion batteries. This paper is concluded with an outlook on future work in Sec. 5.

Throughout the paper, the following set of notations is used: The transpose of a matrix $\boldsymbol{M}$ is denoted by $\boldsymbol{M}^T$, its conjugate is $\bar{\boldsymbol{M}}$ and its conjugate transpose $\boldsymbol{M}^H$. $\mathrm{Sym}\{\boldsymbol{M}\}$ means $\boldsymbol{M} + \boldsymbol{M}^H$. The left and right endpoints of an interval $[\boldsymbol{x}]$ are denoted respectively by $\underline{\boldsymbol{x}}$ and $\overline{\boldsymbol{x}}$ such that $[\boldsymbol{x}] = [\underline{\boldsymbol{x}}\ ;\ \overline{\boldsymbol{x}}]$. For any two vectors $\boldsymbol{x}_1, \boldsymbol{x}_2$ or matrices $\boldsymbol{M}_1, \boldsymbol{M}_2$, the relations $\boldsymbol{x}_1 \leq \boldsymbol{x}_2$ and $\boldsymbol{M}_1 \leq \boldsymbol{M}_2$ are understood element-wise. The relation $\boldsymbol{M} \prec 0$ ($\boldsymbol{M} \succ 0$) means that the matrix $\boldsymbol{M} \in \mathbb{C}^{n\times n}$ is negative (positive) definite. The symbol $\boldsymbol{I}$ denotes the identity matrix.

2. PRELIMINARIES

In this paper, commensurate FLTI systems are considered permitting a state-space representation

$$\begin{cases} \mathcal{D}_t^\gamma \boldsymbol{x}(t) = \boldsymbol{A}\boldsymbol{x}(t) + \boldsymbol{B}\boldsymbol{u}(t) + \boldsymbol{E}\boldsymbol{z}(t), & \boldsymbol{x}(t_0) = \boldsymbol{x}_0 \\ \boldsymbol{y}(t) = \boldsymbol{C}\boldsymbol{x}(t) + \boldsymbol{D}\boldsymbol{u}(t) + \boldsymbol{F}\boldsymbol{z}(t), & \gamma \in (0,2) \end{cases} \tag{1}$$

with the state vector $\boldsymbol{x}(t) \in \mathbb{R}^n$, the input vector $\boldsymbol{u} \in \mathbb{R}^p$, the output vector $\boldsymbol{y}(t) \in \mathbb{R}^m$, and the disturbance input vector $\boldsymbol{z}(t) \in \mathbb{R}^q$. Additionally, $\boldsymbol{A}$, $\boldsymbol{B}$, $\boldsymbol{C}$, $\boldsymbol{D}$, $\boldsymbol{E}$, and $\boldsymbol{F}$ are constant real matrices. $\mathcal{D}^\gamma$ is the fractional differentiation operator of order γ, whereby the presented results are valid regardless of the definition used, e.g. Grünwald-Letnikov, Riemann-Liouville, Caputo etc. (Podlubny, 1999). The transfer function matrix between $\boldsymbol{u}(t)$ and $\boldsymbol{y}(t)$ is $\boldsymbol{H}(s) = \boldsymbol{C}(s^\gamma \boldsymbol{I} - \boldsymbol{A})^{-1}\boldsymbol{B} + \boldsymbol{D}$.

The properties of controllability and observability influence the solvability of control problems significantly. In Monje et al. (2010), it was shown that, as with LTI systems, a necessary and sufficient criterion for the controllability and observability exists, mainly depending on the structure of the analyzed system.

Theorem 1. An FLTI system of the form (1) is fully controllable if and only if the controllability matrix

$$\boldsymbol{Q}_C = \begin{bmatrix} \boldsymbol{B} & \boldsymbol{A}\boldsymbol{B} & \boldsymbol{A}^2\boldsymbol{B} & \ldots & \boldsymbol{A}^{n-1}\boldsymbol{B} \end{bmatrix} \tag{2}$$

satisfies the condition $\mathrm{rank}\{\boldsymbol{Q}_C\} = n$.

Theorem 2. An FLTI system of the form (1) is fully observable if and only if the observability matrix

$$\boldsymbol{Q}_O = \begin{bmatrix} \boldsymbol{C}^T & (\boldsymbol{C}\boldsymbol{A})^T & (\boldsymbol{C}\boldsymbol{A}^2)^T & \ldots & (\boldsymbol{C}\boldsymbol{A}^{n-1})^T \end{bmatrix}^T \tag{3}$$

satisfies the condition $\mathrm{rank}\{\boldsymbol{Q}_O\} = n$.

Throughout the paper, the dynamic system is always assumed to be fully controllable and observable. Stability in terms of the location of eigenvalues, is checked by extended the well-known stability domain of LTI systems (the complex left half-plane) to the more general commensurate FLTI case, cf. Sabatier and Farges (2012).

Theorem 3. The system (1) is asymptotically stable if and only if the following condition is satisfied

$$\left|\arg(\mathrm{eig}(\boldsymbol{A}))\right| > \gamma\frac{\pi}{2}, \quad \gamma \in (0,2), \tag{4}$$

where $\mathrm{eig}(\boldsymbol{A})$ represents the set of all eigenvalues of the matrix $\boldsymbol{A}$. A corresponding graphical interpretation of the stability region is shown in the shaded areas in Fig. 1.

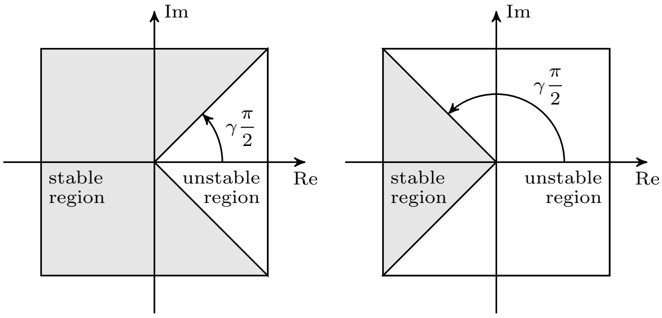

(a) Order: $\gamma \in (0,1)$. (b) Order: $\gamma \in [1,2)$.

Fig. 1. Stability regions of FLTI systems.

In this paper, LMIs are used to verify and ensure the global asymptotic stability of uncertain systems. Alongside Lyapunov's method, the bounded real lemma forms the basis of many LMI approaches in robust control. Although the bounded real lemma is used in both, linear and nonlinear control engineering, the actual result is based on the state-space representation of an LTI system (partially after overbounding nonlinear dynamics). The worst case performance of a stable system measured in terms of the maximum amplification between the input and output is quantified by the $\mathcal{H}_\infty$ norm

$$\|\boldsymbol{H}(s)\|_\infty = \sup_{\mathrm{Re}(s)>0} \overline{\delta}(\boldsymbol{H}(s)) = \sup_{\omega\in\mathbb{R}} \overline{\delta}(\boldsymbol{H}(j\omega)), \tag{5}$$

where $\overline{\delta}$ denotes the maximum singular value. The $\mathcal{H}_\infty$ norm for an integer-order system can be written in terms of an LMI. The result is called the bounded real lemma, see VanAntwerp and Braatz (2000).

Theorem 4. Let $\mu > 0$ be a given real number and the order of the system (1) be $\gamma = 1$. Then $\|\boldsymbol{H}(s)\|_\infty < \mu$ is equivalent to the existence of a symmetric matrix $\exists \boldsymbol{P} = \boldsymbol{P}^T \in \mathbb{R}^{n\times n}$ satisfying the LMIs

$$\begin{bmatrix} \boldsymbol{P}\boldsymbol{A} + \boldsymbol{A}^T\boldsymbol{P} & \boldsymbol{P}\boldsymbol{B} & \boldsymbol{C}^T \\ \boldsymbol{B}^T\boldsymbol{P} & -\mu\boldsymbol{I} & \boldsymbol{D}^T \\ \boldsymbol{C} & \boldsymbol{D} & -\mu\boldsymbol{I} \end{bmatrix} \prec 0, \quad \boldsymbol{P} \succ 0. \tag{6}$$

Moreover, LMIs can be used to test whether the eigenvalues of a matrix belong to a specific area in the complex plane. Thus, existing approaches do not try to extend the bounded real lemma to FLTI systems of the form (1), but rather to find conditions describing the stability region in terms of performance requirements such as damping ratios, cf. Chilali et al. (1999), in Fig. 1.

Theorem 5. Let $\mu > 0$ be a given real number and the fractional order of the system (1) be in the range of $\gamma \in [1,2)$. Then, $\|\boldsymbol{H}(s)\|_\infty < \mu$ is equivalent to the existence of a Hermitian matrix $\exists \boldsymbol{P} = \boldsymbol{P}^H \in \mathbb{C}^{n\times n}$ satisfying the LMIs

$$\begin{bmatrix} r\boldsymbol{P}\boldsymbol{A} + \bar{r}\boldsymbol{A}^T\boldsymbol{P} & r\boldsymbol{P}\boldsymbol{B} & \boldsymbol{C}^T \\ \bar{r}\boldsymbol{B}^T\boldsymbol{P} & -\mu\boldsymbol{I} & \boldsymbol{D}^T \\ \boldsymbol{C} & \boldsymbol{D} & -\mu\boldsymbol{I} \end{bmatrix} \prec 0, \quad \boldsymbol{P} \succ 0, \tag{7}$$

where $r = e^{j(1-\gamma)\frac{\pi}{2}}$ and $\bar{r} = e^{-j(1-\gamma)\frac{\pi}{2}}$.

In contrast, the description of the stability region for the case $\gamma \in (0,1)$ is anything but trivial. The main issue when dealing with LMIs is the convexity of the optimization problem. Briefly, a set is said to be convex if for two points belonging to the set the connecting line is also contained in the respective set. Fig. 1 shows that for the order $\gamma \in (0,1)$ the set of eigenvalues is not convex. To solve this problem, there are different approaches. The most promising for control engineering is based on a decomposition of the stability region. For more details, see Sabatier et al. (2010).

Theorem 6. Let $\mu > 0$ be a given real number and the fractional order of the system (1) be in the range of $\gamma \in (0,1)$. Then, $\|\boldsymbol{H}(s)\|_\infty < \mu$ is equivalent to the existence of the Hermitian matrices $\exists \boldsymbol{P}_1 = \boldsymbol{P}_1^H \in \mathbb{C}^{n\times n}$, $\exists \boldsymbol{P}_2 = \boldsymbol{P}_2^H \in \mathbb{C}^{n\times n}$ satisfying the LMIs

$$\begin{bmatrix} \mathrm{Sym}\{(r\boldsymbol{P}_1 + \bar{r}\boldsymbol{P}_2)\boldsymbol{A}\} & (r\boldsymbol{P}_1 + \bar{r}\boldsymbol{P}_2)\boldsymbol{B} & \boldsymbol{C}^T \\ \boldsymbol{B}^T(r\boldsymbol{P}_1 + \bar{r}\boldsymbol{P}_2)^H & -\mu\boldsymbol{I} & \boldsymbol{D}^T \\ \boldsymbol{C} & \boldsymbol{D} & -\mu\boldsymbol{I} \end{bmatrix} \prec 0, \quad \boldsymbol{P}_1 \succ 0, \quad \boldsymbol{P}_2 \succ 0\ . \tag{8}$$

The LMI conditions to analyze stability of FLTI systems in Theorems 5 and 6 are obtained by a congruence transformation of those given in Farges et al. (2013) under consideration of identical feasible solution sets.

3. FRACTIONAL-ORDER OBSERVER DESIGN

In this section, the LMI conditions for the $\mathcal{H}_\infty$ control synthesis by Farges et al. (2013), see the previous section, are transferred to the dual task of observer synthesis. Then, a novel additional condition is introduced to ensure cooperativity of the error dynamics before applying it to the design of a robust observer for Lithium-Ion batteries.

3.1 Observer Synthesis for Point-Valued Systems

A state observer for an FLTI system (1) is defined as

$$\begin{cases} \mathcal{D}_t^\gamma \hat{\boldsymbol{x}}(t) = \boldsymbol{A}\hat{\boldsymbol{x}}(t) + \boldsymbol{B}\boldsymbol{u}(t) + \boldsymbol{L}(\boldsymbol{y}_m(t) - \hat{\boldsymbol{y}}(t)) \\ \hat{\boldsymbol{y}}(t) = \boldsymbol{C}\hat{\boldsymbol{x}}(t) + \boldsymbol{D}\boldsymbol{u}(t) \end{cases} \tag{9}$$

with the estimated state vector $\hat{\boldsymbol{x}}(t)$, the estimated output vector $\hat{\boldsymbol{y}}(t)$, and the measurement $\boldsymbol{y}_m(t)$. Therefore, the estimation error dynamics have the following form

$$\begin{cases} \mathcal{D}_t^\gamma \tilde{\boldsymbol{x}}(t) = (\boldsymbol{A} - \boldsymbol{L}\boldsymbol{C})\tilde{\boldsymbol{x}}(t) + (\boldsymbol{E} - \boldsymbol{L}\boldsymbol{F})\boldsymbol{z}(t) \\ \tilde{\boldsymbol{y}}(t) = \boldsymbol{C}\tilde{\boldsymbol{x}}(t) + \boldsymbol{F}\boldsymbol{z}(t)\ , \end{cases} \tag{10}$$

where $\tilde{\boldsymbol{x}}(t) = \boldsymbol{x}(t) - \hat{\boldsymbol{x}}(t)$ and $\tilde{\boldsymbol{y}}(t) = \boldsymbol{y}_m(t) - \hat{\boldsymbol{y}}(t)$.

The aim of the $\mathcal{H}_\infty$ observer is to determine a constant observer gain $\boldsymbol{L}$ such that the estimation error dynamics are asymptotically stable according to the stability criterion (4) and that the $\mathcal{H}_\infty$ norm of the transfer function between $\boldsymbol{z}(t)$ and $\tilde{\boldsymbol{y}}(t)$

$$\boldsymbol{G}(s) = \boldsymbol{C}\left(s^\gamma \boldsymbol{I} - (\boldsymbol{A} - \boldsymbol{L}\boldsymbol{C})\right)^{-1}(\boldsymbol{E} - \boldsymbol{L}\boldsymbol{F}) + \boldsymbol{F} \tag{11}$$

is less than a given real number $\mu > 0$. To solve the synthesis problem, the following LMIs are obtained.

Theorem 7. For an FLTI system (9) of order $\gamma \in [1,2)$, there exists a stabilizing observer gain $\boldsymbol{L}$ with $\|\boldsymbol{G}(s)\|_\infty < \mu$, if matrices $\exists \boldsymbol{X} = \boldsymbol{X}^T \in \mathbb{R}^{n\times n}$ and $\exists \boldsymbol{Y} \in \mathbb{R}^{n\times m}$ exist such that the following LMIs hold

$$\begin{bmatrix} \mathrm{Sym}\{r\boldsymbol{X}\boldsymbol{A} - r\boldsymbol{Y}\boldsymbol{C}\} & r\boldsymbol{X}\boldsymbol{E} - r\boldsymbol{Y}\boldsymbol{F} & \boldsymbol{C}^T \\ \boldsymbol{E}^T\bar{r}\boldsymbol{X} - \boldsymbol{F}^T\bar{r}\boldsymbol{Y}^T & -\mu\boldsymbol{I} & \boldsymbol{F}^T \\ \boldsymbol{C} & \boldsymbol{F} & -\mu\boldsymbol{I} \end{bmatrix} \prec 0, \quad \boldsymbol{X} \succ 0, \quad \mu > 0\ . \tag{12}$$

If a feasible solution exists, the observer gain is given by

$$\boldsymbol{L} = \boldsymbol{X}^{-1}\boldsymbol{Y}, \quad \boldsymbol{L} \in \mathbb{R}^{n\times m}\ . \tag{13}$$

Theorem 8. For an FLTI system (9) of order $\gamma \in (0,1)$, there exists a stabilizing observer gain $\boldsymbol{L}$ with $\|\boldsymbol{G}(s)\|_\infty < \mu$, if matrices $\exists \boldsymbol{X} = \boldsymbol{X}^H \in \mathbb{C}^{n\times n}$ and $\exists \boldsymbol{Y} \in \mathbb{R}^{n\times m}$ exist such that the following LMIs hold

$$\begin{bmatrix} \mathrm{Sym}\{(r\boldsymbol{X} + \bar{r}\bar{\boldsymbol{X}})\boldsymbol{A} - \boldsymbol{Y}\boldsymbol{C}\} & * & * \\ \boldsymbol{E}^T(r\boldsymbol{X} + \bar{r}\bar{\boldsymbol{X}})^T - \boldsymbol{F}^T\boldsymbol{Y}^T & -\mu\boldsymbol{I} & * \\ \boldsymbol{C} & \boldsymbol{F} & -\mu\boldsymbol{I} \end{bmatrix} \prec 0, \quad \boldsymbol{X} \succ 0, \quad \mu > 0\ . \tag{14}$$

If a feasible solution exists, the observer gain is calculated by

$$\boldsymbol{L} = (r\boldsymbol{X} + \bar{r}\bar{\boldsymbol{X}})^{-1}\boldsymbol{Y}, \quad \boldsymbol{L} \in \mathbb{R}^{n\times m}. \tag{15}$$

Here, Theorems 7 and 8 are obtained directly from Theorems 5 and 6 by exploiting the duality between control and observer design, namely, by replacing $\boldsymbol{A}$ with $\boldsymbol{A} - \boldsymbol{L}\boldsymbol{C}$, $\boldsymbol{B}$ with $\boldsymbol{E} - \boldsymbol{L}\boldsymbol{F}$ and $\boldsymbol{D}$ with $\boldsymbol{F}$, and using the linearizing changes of variables $\boldsymbol{Y} = \boldsymbol{X}\boldsymbol{L}$ for Theorem 7 and $\boldsymbol{Y} = (r\boldsymbol{X} + \bar{r}\bar{\boldsymbol{X}})\boldsymbol{L}$ for Theorem 8.

Note, for Theorem 7 the matrix variable $\boldsymbol{P} = \boldsymbol{X}$ is restricted to purely real-valued entries to generate a real-valued observer gain $\boldsymbol{L}$. A certain conservatism is then expected in the LMI condition. For Theorem 8, the matrix variable $\boldsymbol{P}_1 = \boldsymbol{X}$ remains complex. However, by defining the matrix variable $\boldsymbol{P}_2 = \bar{\boldsymbol{X}}$ as the conjugate of $\boldsymbol{P}_1$, a real observer gain $\boldsymbol{L}$ is generated because $r\boldsymbol{X} + \bar{r}\bar{\boldsymbol{X}}$ and, hence, $\boldsymbol{Y}$ are both real matrices. Here, it was proven by Farges et al. (2010) that there is no additional conservatism.

3.2 Interval Observer Synthesis

For an FLTI system (1), an interval observer consisting of two conventional observers — one for each bound —, is defined as

$$\begin{cases} \mathcal{D}_t^\gamma \underline{\boldsymbol{x}}(t) = \boldsymbol{A}\underline{\boldsymbol{x}}(t) + \boldsymbol{B}\boldsymbol{u}(t) + \boldsymbol{L}(\boldsymbol{y}_m(t) - \underline{\boldsymbol{y}}(t)) \\ \mathcal{D}_t^\gamma \overline{\boldsymbol{x}}(t) = \boldsymbol{A}\overline{\boldsymbol{x}}(t) + \boldsymbol{B}\boldsymbol{u}(t) + \boldsymbol{L}(\boldsymbol{y}_m(t) - \overline{\boldsymbol{y}}(t)) \\ \underline{\boldsymbol{x}}(t_0) = \underline{\boldsymbol{x}}_0, \quad \overline{\boldsymbol{x}}(t_0) = \overline{\boldsymbol{x}}_0 \end{cases} \tag{16}$$

with the output equations

$$\begin{cases} \underline{\boldsymbol{y}}(t) = \boldsymbol{C}\underline{\boldsymbol{x}}(t) + \boldsymbol{D}\boldsymbol{u}(t) \\ \overline{\boldsymbol{y}}(t) = \boldsymbol{C}\overline{\boldsymbol{x}}(t) + \boldsymbol{D}\boldsymbol{u}(t) \end{cases}, \tag{17}$$

where $\underline{\boldsymbol{x}}(t), \overline{\boldsymbol{x}}(t)$ and $\underline{\boldsymbol{y}}(t), \overline{\boldsymbol{y}}(t)$ are the estimated lower as well as upper bounds of the state and output vectors, respectively, and $\boldsymbol{y}_m(t)$ characterizes the measurement. The objective of this interval observer is to compute two sets of trajectories $\underline{\boldsymbol{x}}(t)$ and $\overline{\boldsymbol{x}}(t)$, such that starting from an initial domain $\underline{\boldsymbol{x}}_0 \leq \boldsymbol{x}_0 \leq \overline{\boldsymbol{x}}_0$ the true state $\boldsymbol{x}(t)$ is always guaranteed to be included by

$$\underline{\boldsymbol{x}}(t) \leq \boldsymbol{x}(t) \leq \overline{\boldsymbol{x}}(t), \quad \forall t > 0. \tag{18}$$

This condition is satisfied if an observer gain $\boldsymbol{L}$ can be found so that the system matrix $\boldsymbol{A} - \boldsymbol{L}\boldsymbol{C}$ is asymptotically stable according to (4) and simultaneously satisfies the property of being a Metzler matrix, see Raïssi and Efimov (2018). Determining the observer gain on the basis of Theorems 7 and 8 is possible by means of LMIs. For uncertain systems given by intervals in either of their system matrices, the LMIs are evaluated for a joint solution including all vertex matrices of a polytopic description.

Theorem 9. For the FLTI system (16) of order $\gamma \in [1, 2)$, there exists an observer gain $\boldsymbol{L}$, if a diagonal matrix $\exists \boldsymbol{Z} \in \mathbb{R}^{n\times n}$ and a matrix $\exists \boldsymbol{Y} \in \mathbb{R}^{n\times m}$ exist, such that the following LMIs hold

$$\begin{bmatrix} \mathrm{Sym}\{r\boldsymbol{ZA} - r\boldsymbol{YC}\} & r\boldsymbol{ZE} - r\boldsymbol{YF} & \boldsymbol{C}^T \\ \boldsymbol{E}^T\bar{r}\boldsymbol{Z} - \boldsymbol{F}^T\bar{r}\boldsymbol{Y}^T & -\mu\boldsymbol{I} & \boldsymbol{F}^T \\ \boldsymbol{C} & \boldsymbol{F} & -\mu\boldsymbol{I} \end{bmatrix} \prec 0, \qquad (19)$$
$$\boldsymbol{ZA} - \boldsymbol{YC} + \kappa\boldsymbol{Z} \geq 0, \quad \boldsymbol{Z} \succ 0, \quad \mu > 0,$$

where a sufficiently large value κ has to be given. If a feasible solution exists, the observer gain is calculated according to

$$\boldsymbol{L} = \boldsymbol{Z}^{-1}\boldsymbol{Y}, \quad \boldsymbol{L} \in \mathbb{R}^{n\times m}. \qquad (20)$$

Theorem 10. For the FLTI system (16) of order $\gamma \in (0, 1)$, there exists an observer gain $\boldsymbol{L}$, if a diagonal matrix $\exists \boldsymbol{Z} \in \mathbb{R}^{n\times n}$ and a matrix $\exists \boldsymbol{Y} \in \mathbb{R}^{n\times m}$ exist, such that the following LMIs hold

$$\begin{bmatrix} \mathrm{Sym}\{(r\boldsymbol{Z} + \bar{r}\boldsymbol{Z})\boldsymbol{A} - \boldsymbol{YC}\} & * & * \\ \boldsymbol{E}^T(r\boldsymbol{Z} + \bar{r}\boldsymbol{Z})^T - \boldsymbol{F}^T\boldsymbol{Y}^T & -\mu\boldsymbol{I} & * \\ \boldsymbol{C} & \boldsymbol{F} & -\mu\boldsymbol{I} \end{bmatrix} \prec 0, \qquad (21)$$
$$(r\boldsymbol{Z} + \bar{r}\boldsymbol{Z})\boldsymbol{A} - \boldsymbol{YC} + (r\boldsymbol{Z} + \bar{r}\boldsymbol{Z})\kappa \geq 0,\ \boldsymbol{Z} \succ 0,\ \mu > 0,$$

where a sufficiently large value κ has to be given. If a feasible solution exists, the observer gain is calculated by

$$\boldsymbol{L} = (r\boldsymbol{Z} + \bar{r}\boldsymbol{Z})^{-1}\boldsymbol{Y}, \quad \boldsymbol{L} \in \mathbb{R}^{n\times m}. \qquad (22)$$

To ensure the Metzler property of the system matrix, the following inequality constraint can be formulated

$$(\boldsymbol{A} - \boldsymbol{LC}) + \kappa\boldsymbol{I} \geq 0. \qquad (23)$$

Note that the term $\kappa\boldsymbol{I}$ is added to the Metzler constraint, since only off-diagonal elements of the matrix must be nonnegative. To eliminate the bilinearity caused by inserting (20) or (22) in (23), $\boldsymbol{Z}$ is restricted to being diagonal.

4. APPLICATION SCENARIO: BATTERY SYSTEMS

To evaluate the efficiency of the proposed method, it is implemented for estimating the SOC of a Lithium-Ion battery. Since the required estimation model should capture the battery dynamics with sufficient accuracy and have a simple structure to reduce computing times, the mathematical modeling by means of an equivalent circuit was adopted. This is motivated by an electro-chemical impedance spectroscopy and attempts to describe experimentally measured impedance data using electrical elements. By using fractional calculus, a generalized capacitive element

$$Z_{\mathrm{CPE}}(\omega) = \frac{1}{Q(j\omega)^\gamma}, \quad \gamma \in (0, 1), \qquad (24)$$

of the fractional order γ with the pseudo capacitance Q is introduced. The additional degree of freedom in the differential order γ allows the model to predict the electrical behavior of a battery more accurately than in the case of a purely integer-order system representation. A fractional equivalent circuit model[1] is shown in Fig. 2. For more details, see Zou et al. (2018) and Andre et al. (2011).

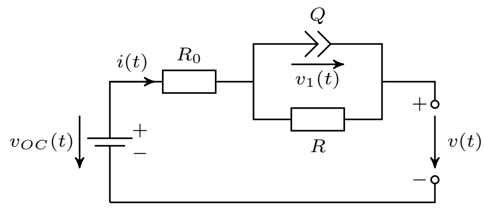

Fig. 2. Typical fractional-order equivalent circuit model.

Considering the Lithium-Ion battery model in Fig. 2, the following governing equations can be formulated based on Kirchhoff's current and voltage laws

$$\begin{cases} \mathcal{D}_t^1\sigma(t) = -\dfrac{\eta}{3600C_N}, \\ \mathcal{D}_t^\gamma v_1(t) = -\dfrac{1}{RQ}v_1(t) + \dfrac{1}{Q}i(t), \\ \quad v(t) = \ v_{OC}(t) - v_1(t) - R_0 i(t), \end{cases} \qquad (25)$$

where $\sigma(t) \in (0, 1)$ describes the SOC, $i(t)$ the input current and $v(t)$ the terminal voltage of the battery. Additionally, R_0, R, and Q are the lumped circuit element parameters, η the Coulomb efficiency, and C_N the nominal capacity in Ah. Furthermore, for the nonlinear characteristics of the open-circuit voltage, it was assumed that

$$v_{OC}(t) = \sum_{k=0}^{4} c_k\sigma^k(t) + d_0 e^{d_1\sigma(t)}i(t), \qquad (26)$$

according to the observations of Hu et al. (2012), holds. The observer's design presupposes a commensurate and quasi-linear form. To reduce the complexity of the model, the fractional derivative order of the model is set to $\gamma = 0.5$ complying with a previous parameter identification. This leads to the state-space representation

$$\begin{cases} \mathcal{D}_t^{0.5}\boldsymbol{x}(t) = \boldsymbol{Ax}(t) + \boldsymbol{B}i(t) \\ \quad v(t) = \boldsymbol{C}(\sigma(t))\boldsymbol{x}(t) + D(\sigma(t))i(t) \\ \quad \boldsymbol{x}(t_0) = \boldsymbol{x}_0 \in \mathbb{R}^3\ , \end{cases} \qquad (27)$$

with the state vector $\boldsymbol{x}(t) = \begin{bmatrix}\sigma(t) & \mathcal{D}_t^{0.5}\sigma(t) & v_1(t)\end{bmatrix}^T$, the system matrices

$$\boldsymbol{A} = \begin{bmatrix} 0 & 1 & 0 \\ 0 & 0 & 0 \\ 0 & 0 & -\frac{1}{RQ} \end{bmatrix}, \quad \boldsymbol{B} = \begin{bmatrix} 0 \\ -\frac{\eta}{3600C_N} \\ \frac{1}{Q} \end{bmatrix}, \quad \text{and}$$
$$\boldsymbol{C}(\sigma(t)) = \begin{bmatrix} \sum_{k=0}^{4} c_k\sigma^{k-1}(t) & 0 & -1 \end{bmatrix}$$

as well as the feedthrough term $D(\sigma(t)) = -R_0 + d_0 e^{d_1\sigma(t)}$. Table 1 lists the parameter values under consideration, which were identified on the basis of the measurement data published by Reuter et al. (2016).

Table 1. Parameters of the Lithium-Ion battery model.

R_0 [Ω]	Q [F/s$^{0.5}$]	R [Ω]	η [−]	C_N [Ah]	c_0 [V]
$+1.7e^{-5}$	+20.591	+0.1005	+1.0000	+3.1000	+3.0607

c_1 [V]	c_2 [V]	c_3 [V]	c_4 [V]	d_0 [Ω]	d_1 [−]
+3.2965	−8.3942	+11.088	−4.8992	−0.2477	−14.302

[1] Note that additional (generalized) capacitive elements can be included via a series connection similar to Erdinc et al. (2009).

Here, the uncertainty of the system model lies within the variability of the SOC. Hence, the terms in the system's output equation depending on it are replaced by the two reasonably chosen and independent parameter intervals

$$\begin{aligned} \sum_{k=0}^{4} c_k \sigma^{k-1}(t) \quad &\in [p_1] = [1, 250] \text{ and} \\ -R_0 + d_0 e^{d_1 \sigma(t)} &\in [p_2] = [-0.25, 0], \end{aligned} \tag{28}$$

so that the parameter-dependent output vector and feedthrough factor

$$\begin{aligned} \boldsymbol{C}(\sigma(t)) &\in \boldsymbol{C}([p_1]) = \big[[p_1]\ 0\ -1\big] \text{ and} \\ D(\sigma(t)) &\in D([p_2]) = [p_2] \end{aligned} \tag{29}$$

are obtained. Thus, the system behavior is described by $N = 2^2$ vertex matrices forming the polytopic representation. To estimate the SOC $\sigma(t)$ of the Lithium-Ion battery system (27), the nonlinear state observer

$$\begin{cases} \mathcal{D}^{0.5}\hat{\boldsymbol{x}}(t) = \boldsymbol{A}\hat{\boldsymbol{x}}(t) + \boldsymbol{B}i(t) + \boldsymbol{L}(v_m(t) - \hat{v}(t)), \\ \hat{v}(t) = \boldsymbol{C}(\hat{\sigma}(t))\hat{\boldsymbol{x}}(t) + D(\hat{\sigma}(t))i(t), \\ \hat{\boldsymbol{x}}(t_0) = \hat{\boldsymbol{x}}_0, \end{cases} \tag{30}$$

is proposed with the vector of the estimated states $\hat{\boldsymbol{x}}(t)$, the estimated terminal voltage $\hat{v}(t)$, and the measured terminal voltage $v_m(t)$.

Solving the LMIs formulated in Theorem 8 for all $N = 2^2$ vertex matrices with the MATLAB toolboxes YALMIP and MOSEK yields the constant observer gain

$$\boldsymbol{L} = \big[0.0098\ 0.0003\ -0.0309\big]^T \tag{31}$$

for $\mu = 1.5423$ according to Eq. (15). Here, $\boldsymbol{E} = \boldsymbol{B}$ and $\boldsymbol{F} = \boldsymbol{D}$ were chosen for an appropriate weighting of external disturbances. To demonstrate the efficiency of the observer, the initial SOC was disturbed. Fig. 3 illustrates a comparison of measurements and the estimated terminal voltage as well as a comparison of a reference SOC generated by a simulation on the basis of measurements and the estimated SOC for the initial conditions

$$\boldsymbol{x}_0 = \big[0.90\ 0.00\ 0.00\big]^T,\ \hat{\boldsymbol{x}}_0 = \big[0.75\ 0.00\ 0.00\big]^T. \tag{32}$$

The upper graph shows the time evolution of the discharge-recharge current used as input. For the numerical solution of the fractional-order differential equations, the MATLAB routines of Garrappa (2018) were utilised. Since the previous observer design neglected possible disturbances and variations of the battery parameters due to changing operating conditions, a robust interval observer is designed, which additionally allows for estimating guaranteed lower and upper bounds of the SOC and the terminal voltage. For the efficient implementation, the structural property of cooperative systems is exploited. For the design, it was assumed that the occurring disturbances and parameter uncertainties are not exactly known, but lie within a-priori given, finitely large bounds. The resulting quantifiable ranges were added to the measured terminal voltage, yielding the following measurement interval

$$v_m(t) \in [\underline{v}_m, \overline{v}_m](t) = v_m(t) + [-\Delta v_m, +\Delta v_m], \tag{33}$$

so that the true voltage is guaranteed to be within this interval. Under the previous assumptions, the interval observer for the Lithium-Ion battery system (27) is defined as

$$\begin{cases} \mathcal{D}_t^{0.5}\underline{\boldsymbol{x}}(t) = \boldsymbol{A}\underline{\boldsymbol{x}}(t) + \boldsymbol{B}i(t) + \boldsymbol{L}(\underline{v}_m(t) - \underline{v}(t)), \\ \mathcal{D}_t^{0.5}\overline{\boldsymbol{x}}(t) = \boldsymbol{A}\overline{\boldsymbol{x}}(t) + \boldsymbol{B}i(t) + \boldsymbol{L}(\overline{v}_m(t) - \overline{v}(t)), \\ \underline{\boldsymbol{x}}(t_0) = \underline{\boldsymbol{x}}_0, \quad \overline{\boldsymbol{x}}(t_0) = \overline{\boldsymbol{x}}_0, \end{cases} \tag{34}$$

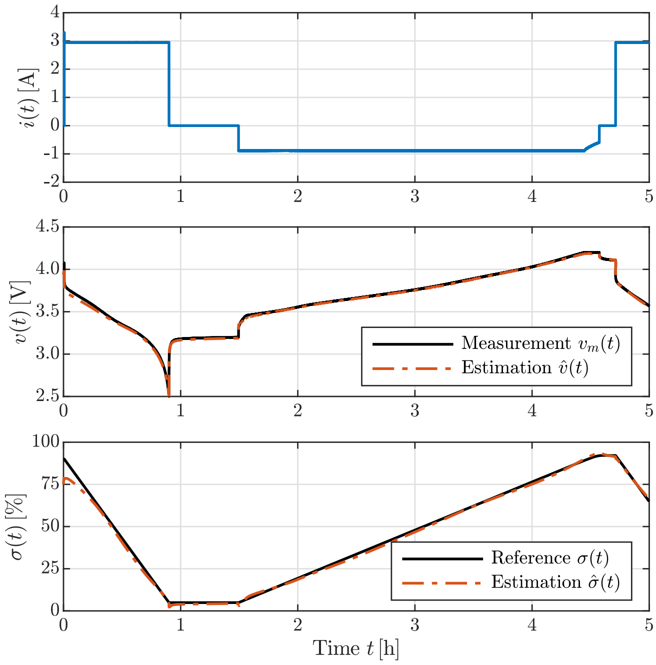

Fig. 3. Result of the state observer for estimating the SOC.

with both output equations

$$\begin{cases} \underline{v}(t) = \underline{\boldsymbol{C}}(\underline{\sigma}(t))\underline{\boldsymbol{x}}(t) + \underline{D}(\underline{\sigma}(t))i(t), \\ \overline{v}(t) = \overline{\boldsymbol{C}}(\overline{\sigma}(t))\overline{\boldsymbol{x}}(t) + \overline{D}(\overline{\sigma}(t))i(t). \end{cases} \tag{35}$$

By solving the LMIs formulated in Theorem 10 for all $N = 2^2$ vertex matrices, the jointly computed observer gain is obtained as

$$\boldsymbol{L} = \big[0.02\ 0.00\ 0.00\big]^T \tag{36}$$

for $\boldsymbol{E} = \boldsymbol{B}$, $\boldsymbol{F} = \boldsymbol{D}$, and $\kappa = 5$ according to Eq. (22). Therefore, the resulting system matrix of the estimation error dynamics

$$(\boldsymbol{A} - \boldsymbol{L}\boldsymbol{C}([p_1])) = \begin{bmatrix} [-5.00, -0.02] & 1.00 & 0.02 \\ 0.00 & 0.00 & 0.00 \\ 0.00 & 0.00 & -0.48 \end{bmatrix} \tag{37}$$

fulfills the property of a Metzler matrix. However, the resulting requirement may appear to be too restrictive for the considered model of the battery system, since some eigenvalues of the system matrix cannot be shifted. Despite the resulting loss of observability, this concept still allows for proving detectability and input-to-state stability (ISS) as a less strong requirement, because all eigenvalues are compliant with the stability domains in Fig. 1(a). The results of the interval observer approach for a measurement uncertainty of $\Delta v_m = 0.04$ V and the initial conditions

$$\begin{aligned} \boldsymbol{x}_0 &= \big[0.90\ 0.00\ 0.00\big]^T, \\ \underline{\boldsymbol{x}}_0 = \big[0.85\ 0.00\ 0.00\big]^T&,\ \overline{\boldsymbol{x}}_0 = \big[0.95\ 0.00\ 0.00\big]^T, \end{aligned} \tag{38}$$

which describe an uncertainty of the SOC at the starting point are shown in Fig. 4. These graphs show the measurement of the terminal voltage and the SOC with the respective estimated lower and upper bounds. Note, the same discharge-charge current as in Fig. 3 was used as the system input.

5. CONCLUSIONS AND FUTURE WORK

In this paper, a robust observer for the nonlinear fractional-order system model of a Lithium-Ion battery was designed

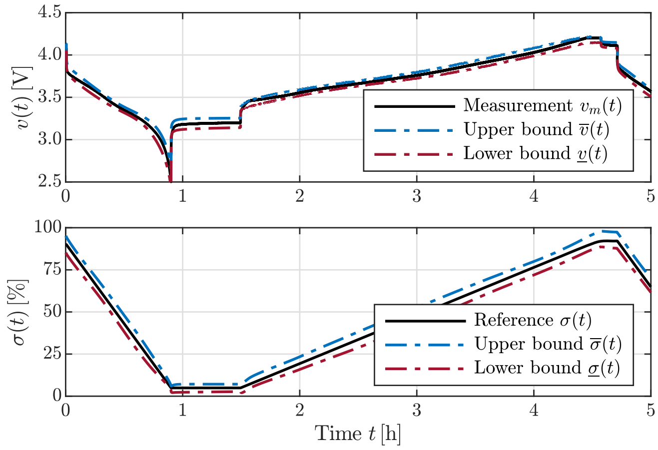

Fig. 4. Result of the interval-based SOC estimation.

to estimate the SOC. Global asymptotic stability (respectively, ISS) of the estimation error dynamics was ensured on the basis of LMIs. While the LMIs for a controller synthesis of FLTI systems were mostly known from the literature, the LMIs for the observer synthesis had to be derived on the basis of a congruence transformation. The simulation results showed that the observer is able to accurately reconstruct the SOC.

Based on this, an interval observer was designed which estimates guaranteed upper and lower bounds for the SOC and the terminal voltage. Therefore, an observer gain had to be determined, so that the system matrix of the estimation error dynamics was simultaneously asymptotically stable and ensured the property of a Metzler matrix. A structural analysis showed that these requirements may under some circumstances be too restrictive for the model of a Lithium-Ion battery. Therefore, combining the interval observer synthesis with state-space transformations as in Kersten et al. (2018) and Rauh et al. (2019) is recommended for future work, where these transformations help to fully exploit the benefits of an H_∞ optimization as in the design procedure presented in this paper. This will allow for computing state bounds in an efficient manner, although the result of the observer design may no longer be given directly by cooperative dynamics.

REFERENCES

Andre, D., Meiler, M., Steiner, K., Wimmer, C., Soczka-Guth, T., and Sauer, D.U. (2011). Characterization of High-Power Lithium-Ion Batteries by Electrochemical Impedance Spectroscopy. I. Experimental Investigation. *Journal of Power Sources*, 196(12), 5334–5341.

Chilali, M., Gahinet, P., and Apkarian, P. (1999). Robust Pole Placement in LMI Regions. *IEEE Transactions on Automatic Control*, 44(12), 2257–2270.

Erdinc, O., Vural, B., and Uzunoglu, M. (2009). A Dynamic Lithium-Ion Battery Model Considering the Effects of Temperature and Capacity Fading. In *Proc. of Intl. Conf. on Clean Electrical Power*, 383–386.

Farges, C., Fadiga, L., and Sabatier, J. (2013). $\mathcal{H}_\infty$ Analysis and Control of Commensurate Fractional Order Systems. *Mechatronics*, 23(7), 772–780.

Farges, C., Moze, M., and Sabatier, J. (2010). Pseudo-State Feedback Stabilization of Commensurate Fractional Order Systems. *Automatica*, 46(10), 1730–1734.

Garrappa, R. (2018). Numerical Solution of Fractional Differential Equations: A Survey and a Software Tutorial. *Mathematics*, 6(2), 16.

Hu, X., Li, S., Peng, H., and Sun, F. (2012). Robustness Analysis of State-of-Charge Estimation Methods for two Types of Li-Ion Batteries. *Journal of Power Sources*, 217, 209–219.

Ichalal, D., Marx, B., Maquin, D., and Ragot, J. (2018). State Estimation of System with Bounded Uncertain Parameters: Interval Multimodel Approach. *International Journal of Adaptive Control and Signal Processing*, 32, 480–493.

Kersten, J., Rauh, A., and Aschemann, H. (2018). State-Space Transformations of Uncertain Systems with Purely Real and Conjugate-Complex Eigenvalues into a Cooperative Form. In *2018 23rd Intl. Conf. on Methods & Models in Automation & Robotics (MMAR)*, 797–802.

Monje, C.A., Chen, Y.Q., Vinagre, B.M., Xue, D., and Feliu-Batlle, V. (2010). *Fractional-Order Systems and Controls: Fundamentals and Applications.* Springer Science & Business Media, London.

Oustaloup, A. (1995). *La Dérivation Non Entière: Théorie, Synthèse et Applications.* Hermès. In French.

Podlubny, I. (1999). *Fractional Differential Equations: An Introduction to Fractional Derivatives, Fractional Differential Equations, to Methods of Their Solution and Some of Their Applications.* Academic Press, San Diego.

Raïssi, T. and Aoun, M. (2017). On Robust Pseudo State Estimation of Fractional Order Systems. In *Positive Systems. POSTA 2016. Lecture Notes in Control and Information Sciences*, 97–111. Springer, Cham.

Raïssi, T. and Efimov, D. (2018). Some Recent Results on the Design and Implementation of Interval Observers for Uncertain Systems. *at-Automatisierungstechnik*, 66(3), 213–224.

Rauh, A., Kersten, J., and Aschemann, H. (2019). Techniques for Verified Reachability Analysis of Quasi-Linear Continuous-Time Systems. In *2019 24th Intl. Conf. on Methods & Models in Automation & Robotics (MMAR)*, 18–23.

Reuter, J., Mank, E., Aschemann, H., and Rauh, A. (2016). Battery State Observation and Condition Monitoring Using Online Minimization. In *2016 21st Intl. Conf. on Methods and Models in Automation and Robotics (MMAR)*, 1223–1228.

Sabatier, J. and Farges, C. (2012). On Stability of Commensurate Fractional Order Systems. *International Journal of Bifurcation and Chaos*, 22(04).

Sabatier, J., Moze, M., and Farges, C. (2010). LMI Stability Conditions for Fractional Order Systems. *Computers & Mathematics with Applications*, 59(5), 1594–1609.

VanAntwerp, J.G. and Braatz, R.D. (2000). A Tutorial on Linear and Bilinear Matrix Inequalities. *Journal of Process Control*, 10(4), 363–385.

Wang, B., Liu, Z., Li, S.E., Moura, S.J., and Peng, H. (2017). State-of-Charge Estimation for Lithium-Ion Batteries Based on a Nonlinear Fractional Model. *IEEE Trans. on Control Systems Technology*, 25(1), 3–11.

Zou, C., Zhang, L., Hu, X., Wang, Z., Wik, T., and Pecht, M. (2018). A Review of Fractional-Order Techniques Applied to Lithium-Ion Batteries, Lead-Acid Batteries, and Supercapacitors. *Journal of Power Sources*, 390, 286–296.